

Entanglement Entropy of Two Spheres

Noburo Shiba*

*Department of Physics, Graduate School of Science,
Osaka University, Toyonaka, Osaka 560-0043, Japan*

(Dated: April 3, 2024)

Abstract

We study the entanglement entropy S_{AB} of a massless free scalar field on two spheres A and B whose radii are R_1 and R_2 , respectively, and the distance between the centers of them is r . The state of the massless free scalar field is the vacuum state. We obtain the result that the mutual information $S_{A;B} \equiv S_A + S_B - S_{AB}$ is independent of the ultraviolet cutoff and proportional to the product of the areas of the two spheres when $r \gg R_1, R_2$, where S_A and S_B are the entanglement entropy on the inside region of A and B , respectively. We discuss possible connections of this result with the physics of black holes.

PACS numbers: 03.65.Ud, 04.70.Dy, 11.90.+t

* shiba@het.phys.sci.osaka-u.ac.jp

I. INTRODUCTION

Entanglement entropy in the quantum field theory (QFT) was originally studied to explain black hole entropy [1, 2]. Entanglement entropy is generally defined as the von Neumann entropy $S_A = -\text{Tr} \rho_A \ln \rho_A$ corresponding to the reduced density matrix ρ_A of a subsystem A . When we consider the quantum field theory in $(d+1)$ -dimensional spacetime $\mathbb{R} \times N$, where \mathbb{R} and N denote the time direction and the d -dimensional spacelike manifold, respectively, we define the subsystem by a d -dimensional domain $A \subset N$ at fixed time $t = t_0$. (So this is also called geometric entropy.) Entanglement entropy naturally arises when we consider the black hole because we cannot obtain the information inside the black hole. In fact, in the vacuum state the leading term of the entanglement entropy of A is proportional to the area of the boundary ∂A in many cases [1, 2]. This is similar to black hole entropy, and extensive studies have been carried out [3–8].

In this paper, we study the entanglement entropy S_{AB} of the massless free scalar field in $(d+1)$ -dimensional Minkowski spacetime on two spheres A and B whose radii are R_1 and R_2 and how it depends on the distance r between the centers of the two spheres. Entanglement entropy of two disconnected regions has been studied, see e.g. [9–11]. We consider the case that the state of the massless free scalar field is the vacuum state. We studied S_{AB} in [12] analytically. When $r \gg R_1, R_2$, we obtained the r dependence of S_{AB} as

$$S_{AB} \approx S_A + S_B - \frac{G(R_1, R_2, a)}{r^{2d-2}}, \quad (1)$$

where a is an ultraviolet cutoff length and $G(R_1, R_2, a) = G(R_2, R_1, a) \geq 0$. (Notice that we defined $G(R_1, R_2, a)$ in (1) as that in [12] multiplied by (-1) for simplicity.) We could not determine the functional form of $G(R_1, R_2, a)$. In this paper, we numerically calculate S_{AB} for $d = 2, 3$. We obtain the result that the mutual information $S_{A:B} \equiv S_A + S_B - S_{AB}$ is independent of the ultraviolet cutoff length and $G(R_1, R_2, a)$ is proportional to the simple product of the surface areas of two spheres. (Note that we cannot determine the functional form of $G(R_1, R_2)$ only by the constraints from dimensional analysis, symmetry, and behavior in the limit $R_1 \rightarrow 0$. For example, $G(R_1, R_2) = R_1^3 R_2 + R_1 R_2^3$ is not prohibited by these constraints.) The mutual information is a quantity that measures the entanglement between two systems. (See e.g. [13]) In order to examine whether only the degrees of freedom on the surface of the spheres contribute to the mutual information or not, we calculate the mutual information $S_{D:E}$ of two same spherical shells D and E for $d = 3$ and the mutual information

$S_{H;I}$ of two same rings H and I for $d = 2$. The internal (external) radii of the spherical shell and the ring are L_1 (L_2). The distance between the centers of the two spherical shells and that between the two rings are r . We obtain the result that $S_{D;E}$ and $S_{H;I}$ are monotone decreasing function of L_1 . Then not only the degrees of freedom on the surface of the sphere but also those on the inside region contribute to the mutual information. This result is remarkably different from that of the entanglement entropy to which the degrees of freedom on the surface of the boundary contribute mainly.

Previously, we studied S_{AB} in [12] in order to study an entropic contribution to the force between two black holes. To a distant observer, an object falling into a black hole takes an infinite time to reach the event horizon and the outside region is isolated from the inside region if we neglect the change of the mass of the black hole. Then we are probably able to consider the entanglement entropy of quantum fields on the outside region C of two black holes A and B as thermodynamic entropy, and we can see the entropic force acting on the two black holes from the r dependence of S_C . We consider two systems X and Y , then one can show $S_X = S_Y$ in general if a composite system XY is in a pure state. Then $S_C = S_{AB}$ when the state of the field on the whole space is a pure state. We will roughly estimate the magnitude of the entropic force between two black holes by using S_{AB} in Minkowski spacetime.

The present paper is organized as follows. There have been some computational methods of entanglement entropy [14–16] and the reader is urged to refer to [17–19] for reviews. Among several others, we review in Sec.II the method of Bombelli et al [1] which is most straightforward and suitable for numerical calculations. In Sec.III, we apply the above formalism to a massless free scalar field in $(d + 1)$ -dimensional Minkowski spacetime. We improve the computational method of Bombelli et al to reduce the computational complexity. In Sec.IV, we numerically calculate the entanglement entropy S_{AB} , the mutual information $S_{D;E}$, and $S_{H;I}$ in $(d+1)$ -dimensional Minkowski spacetime for $d = 2, 3$. We roughly estimate the magnitude of the entropic force between two black holes by S_{AB} in $(3+1)$ -dimensional Minkowski spacetime.

II. HOW TO COMPUTE ENTANGLEMENT ENTROPY

In this section we review the computational method developed by Bombelli et al [1]. As a model amenable to unambiguous calculation we deal with the scalar field on \mathbb{R}^d as a collection of coupled oscillators on a lattice of space points, labeled by capital Latin indices, the displacement at each point giving the value of the scalar field there. In this case the Lagrangian can be given by

$$L = \frac{1}{2}G_{MN}\dot{q}^M\dot{q}^N - \frac{1}{2}V_{MN}q^Mq^N, \quad (2)$$

where q^M gives the displacement of the Mth oscillator and \dot{q}^M its generalized velocity. The symmetric matrix G_{MN} is positive definite and therefore invertible; i.e., there exists the inverse matrix G^{MN} such that

$$G^{MP}G_{PN} = \delta^M_N. \quad (3)$$

The matrix V_{MN} is also symmetric and positive definite. The matrices G_{MN} and V_{MN} are independent of q^M and \dot{q}^M . Introducing the conjugate momentum to q^M ,

$$P_M = G_{MN}\dot{q}^N, \quad (4)$$

we can write the Hamiltonian for our system as

$$H = \frac{1}{2}G^{MN}P_MP_N + \frac{1}{2}V_{MN}q^Mq^N. \quad (5)$$

Next, consider the positive definite symmetric matrix W_{MN} defined by

$$W_{MA}G^{AB}W_{BN} = V_{MN}. \quad (6)$$

In this sense the matrix W is the "square root" of V in the scalar product with G .

Now consider a region Ω in \mathbb{R}^d . The oscillators in this region will be specified by Greek letters, and those in the complement of Ω , Ω^c , will be specified by lowercase Latin letters. We will use the following notation

$$W_{AB} = \begin{pmatrix} W_{ab} & W_{a\beta} \\ W_{\alpha b} & W_{\alpha\beta} \end{pmatrix} \equiv \begin{pmatrix} A & B \\ B^T & C \end{pmatrix} \quad W^{AB} = \begin{pmatrix} W^{ab} & W^{a\beta} \\ W^{\alpha b} & W^{\alpha\beta} \end{pmatrix} \equiv \begin{pmatrix} D & E \\ E^T & F \end{pmatrix}, \quad (7)$$

where W^{AB} is the inverse matrix of W_{AB} (W^{AB} is *not* obtained by raising indices with G^{AB}).

So we have

$$\begin{pmatrix} 1 & 0 \\ 0 & 1 \end{pmatrix} = \begin{pmatrix} A & B \\ B^T & C \end{pmatrix} \begin{pmatrix} D & E \\ E^T & F \end{pmatrix} = \begin{pmatrix} AD + BE^T & AE + BF \\ B^TD + CE^T & B^TE + CF \end{pmatrix}. \quad (8)$$

If the information on the displacement of the oscillators in Ω is considered as unavailable, we can obtain a reduced density matrix ρ_{red} for Ω^c , integrating out over $q^\alpha \in \mathbb{R}$ for each of the oscillators in the region Ω , and then we have

$$\rho_{red}(q^a, q'^b) = \int \prod_{\alpha} dq^{\alpha} \rho(q^a, q^{\alpha}, q'^b, q^{\alpha}), \quad (9)$$

where ρ is a density matrix of the total system.

We can obtain the density matrix for the ground state by the standard method, and it is a Gaussian density matrix. Then, ρ_{red} is obtained by a Gaussian integral, and it is also a Gaussian density matrix. The entanglement entropy $S = -\text{tr} \rho_{red} \ln \rho_{red}$ is given by [1]

$$S = \sum_n f(\lambda_n), \quad (10)$$

$$f(\lambda) \equiv \ln\left(\frac{1}{2}\lambda^{1/2}\right) + (1 + \lambda)^{1/2} \ln[(1 + \lambda^{-1})^{1/2} + \lambda^{-1/2}], \quad (11)$$

where λ_n are the eigenvalues of the matrix

$$\Lambda^a_b = -W^{a\alpha}W_{\alpha b} = -(EB^T)^a_b = (DA)^a_b - \delta^a_b. \quad (12)$$

In the last equality we have used (8). The last expression in (12) is useful for numerical calculations when Ω^c is smaller than Ω , because the indices of A and D take over only the space points on Ω^c and the matrix sizes of A and D are smaller than those of B and E . It can be shown that all of λ_n are non-negative as follows. From (8) we have

$$A\Lambda = -AEB^T = BFB^T. \quad (13)$$

It is easy to show that A, C, D and F are positive definite matrices when W and W^{-1} are positive definite matrices. Then $A\Lambda$ is a positive semidefinite matrix as can be seen from (13). So all eigenvalues of Λ are non-negative. After all, we can obtain the entanglement entropy by solving the eigenvalue problem of Λ .

III. LATTICE FORMULATION

We apply the above formalism to a massless free scalar field in $(d + 1)$ -dimensional Minkowski spacetime. The Lagrangian is given by

$$L = \int d^d x \frac{1}{2} [\dot{\phi}^2 - (\nabla\phi)^2]. \quad (14)$$

As an ultraviolet regulator, we replace the continuous d -dimensional space coordinates x by a lattice of discrete points with spacing a . As an infrared cutoff, we allow the individual components of $n \equiv x/a$ to assume only a finite number N of independent values $-N/2 < n_\mu \leq N/2$. The Greek indices denoting vector quantities run from one to d . Outside this range we assume the lattice is periodic. The dimensionless Hamiltonian $H_0 \equiv aH$ is given by

$$H_0 \equiv aH = \sum_n \left[\frac{1}{2} \pi_n^2 + \frac{1}{2} \sum_{\mu=1}^d (\phi_{n_\nu + \delta_{\nu\mu}} - \phi_{n_\nu})^2 + \frac{a^2 m^2}{2} \phi_n^2 \right] \equiv \sum_n \frac{1}{2} \pi_n^2 + \sum_{m,n} \frac{1}{2} \phi_m V_{mn} \phi_n, \quad (15)$$

where ϕ_n and π_n are dimensionless and Hermitian, and obey the canonical commutation relations

$$[\phi_n, \pi_m] = i\delta_{nm}. \quad (16)$$

In Eq.(15) we insert a mass term in order to remove a zero eigenvalue of V_{mn} ; if V_{mn} should have the zero eigenvalue, W^{-1} in (7) would not exist. Later we will take N to infinity. In this limit we can neglect the zero eigenvalue of V_{mn} and will take am to zero. Taking N to infinity is important in order to calculate the entanglement entropy S_{AB} of two spheres. The entanglement entropy of two spheres is more sensitive to the value of N than that of one sphere. (In fact, we numerically calculated S_{AB} for finite N with antiperiodic boundary conditions without the mass term. S_{AB} depends on N when the distance r between two spheres is close to $N/2$, and we could not obtain the clear r dependence of S_{AB} .)

From (15) we obtain (see e.g. [20])

$$W_{mn} = N^{-d} \sum_k [a^2 m^2 + 2 \sum_{\mu=1}^d (1 - \cos \frac{2\pi k_\mu}{N})]^{1/2} e^{2\pi i k(n-m)/N}, \quad (17)$$

$$W_{mn}^{-1} = N^{-d} \sum_k [a^2 m^2 + 2 \sum_{\mu=1}^d (1 - \cos \frac{2\pi k_\mu}{N})]^{-1/2} e^{2\pi i k(n-m)/N}, \quad (18)$$

where the index k also carries d integer valued components, each in the range of $-N/2 < k_\mu \leq N/2$. We take N to infinity and change the momentum sum into an integral with the replacements $q_\mu = 2\pi k_\mu/N$ and $N^{-d} \sum_k \rightarrow \int_{-\pi}^{\pi} \frac{d^d q}{(2\pi)^d}$, and then we have

$$W_{mn} = \int_{-\pi}^{\pi} \frac{d^d q}{(2\pi)^d} e^{iq(n-m)} [a^2 m^2 + 2 \sum_{\mu=1}^d (1 - \cos q_\mu)]^{\frac{1}{2}}, \quad (19)$$

$$W_{mn}^{-1} = \int_{-\pi}^{\pi} \frac{d^d q}{(2\pi)^d} e^{iq(n-m)} [a^2 m^2 + 2 \sum_{\mu=1}^d (1 - \cos q_\mu)]^{\frac{-1}{2}}. \quad (20)$$

In (19) and (20) the integrals converge when $am \rightarrow 0$, so we can take am to zero,

$$W_{mn} = \int_{-\pi}^{\pi} \frac{d^d q}{(2\pi)^d} e^{iq(n-m)} [2 \sum_{\mu=1}^d (1 - \cos q_{\mu})]^{\frac{1}{2}}, \quad (21)$$

$$W_{mn}^{-1} = \int_{-\pi}^{\pi} \frac{d^d q}{(2\pi)^d} e^{iq(n-m)} [2 \sum_{\mu=1}^d (1 - \cos q_{\mu})]^{-\frac{1}{2}}. \quad (22)$$

From (21) and (22) we can compute W_{mn} and W_{mn}^{-1} numerically. Then we can compute the entanglement entropy from (10), (11) and (12). The integrands in (21) and (22) highly oscillate when $\|n - m\| \gg 1$, and the numerical integrals converge very slowly. We can obtain approximate expressions of W_{mn} and W_{mn}^{-1} by hand when $\|n - m\| \gg 1$, so we will use them when $\|n - m\| \gg 1$ in order to reduce the computational complexity of W_{mn} and W_{mn}^{-1} . To evaluate W_{mn} and W_{mn}^{-1} when $\|n - m\| \gg 1$, we define $r \equiv a(n - m)$ and take $\|n - m\|$ to infinity keeping r fixed. We change the variable as $p = q/a$, and then we have

$$W_{mn} = a^d \int_{-\frac{\pi}{a}}^{\frac{\pi}{a}} \frac{d^d p}{(2\pi)^d} e^{ipr} [2 \sum_{\mu=1}^d (1 - \cos ap_{\mu})]^{\frac{1}{2}} \rightarrow a^{d+1} \int_{-\infty}^{\infty} \frac{d^d p}{(2\pi)^d} e^{ipr - \frac{a}{\pi} \|p\|} [\|p\|^2]^{\frac{1}{2}}. \quad (23)$$

We can perform the integral in (23) analytically when $\|r\|/a \rightarrow \infty$ (see Appendix A of [12]), and then we obtain

$$W_{mn} \rightarrow a^{d+1} \frac{A_d}{\|r\|^{d+1}} = \frac{A_d}{\|n - m\|^{d+1}}, \quad (24)$$

where

$$A_d = \begin{cases} -\frac{(d-1)!!}{(2\pi)^{d/2}} & \text{for even } d \geq 2, \\ -2\frac{(d-1)!!}{(2\pi)^{(d+1)/2}} & \text{for odd } d \geq 3. \end{cases} \quad (25)$$

We can evaluate W_{mn}^{-1} when $\|n - m\| \gg 1$ in the same way (see Appendix A of [12]), and then we obtain

$$W_{mn}^{-1} \rightarrow a^{d-1} \int_{-\infty}^{\infty} \frac{d^d p}{(2\pi)^d} e^{ipr - \frac{a}{\pi} \|\vec{p}\|} [\|\vec{p}\|^2]^{-\frac{1}{2}} \rightarrow a^{d-1} \frac{B_d}{\|r\|^{d-1}} = \frac{B_d}{\|n - m\|^{d-1}}. \quad (26)$$

where

$$B_d = \begin{cases} \frac{(d-3)!!}{(2\pi)^{d/2}} & \text{for even } d \geq 2, \\ 2\frac{(d-3)!!}{(2\pi)^{(d+1)/2}} & \text{for odd } d \geq 3, \end{cases} \quad (27)$$

where $0!! = (-1)!! = 1$.

IV. NUMERICAL CALCULATIONS

We calculate numerically the entanglement entropy S_{AB} of two spheres A and B whose radii are R_1 and R_2 , and the distance between the centers of them is r for $d = 3$.

We put the centers of the spheres on a lattice. We define the sphere whose radius is R as a set of points which are at distances of R or less from the center of the sphere. In order to reduce the computational complexity of W_{mn} and W_{mn}^{-1} , we use the approximate expressions (24) and (26) when $\|n - m\| > 10$, and we use the numerical integrals of exact expressions (21) and (22) when $\|n - m\| \leq 10$. When $\|n - m\| = 10$, the differences between the numerical integrals of the exact expressions and the approximate expressions are less than 4% for W_{mn} and less than 1% for W_{mn}^{-1} . We perform matrix operations and calculate the eigenvalues λ_n of the matrix Λ in (12) with **Mathematica** 8. The number of columns and rows of Λ is the number of points in the region of which we calculate entanglement entropy.

We show the computed values of $S(R)$ which is the entanglement entropy of one sphere as a function of R^2/a^2 in Fig.1, where a is a lattice spacing. The points are fitted by a straight line:

$$S = 0.37R^2/a^2. \quad (28)$$

This result agrees with the result in [2] except for the coefficient. (The coefficient in [2] is 0.30. This difference necessarily arises from the difference of regularization methods. In [2] the author use the polar coordinate system and replace the continuous radial coordinate by a lattice.)

We show the computed values of $S_{AB}(r, R_1, R_2)$ which is the entanglement entropy of two spheres as a function of r/a for $R_1/a = R_2/a = 6, 7$ in Fig.2. As can be seen, S_{AB} reaches its maximum value $S_A + S_B$ when $r \rightarrow \infty$. In order to clarify the behavior of S_{AB} as a function of r , we show the computed values of $(S_A + S_B - S_{AB})^{-1/4}(r, R_1, R_2)$ as a function of r/a for $R_1/a = R_2/a = 6, 7$ in Fig.3. The straight lines in Fig.3 are fitted by the data between $r/a = R_1/a + R_2/a + 24$ and $r/a = R_1/a + R_2/a + 84$. In these regions the points are beautifully fitted by the straight lines. Then, when $r \gg R_1, R_2$, we obtain

$$-S_{A;B} \equiv S_{AB}(r, R_1, R_2) - S_A(R_1) - S_B(R_2) \approx -\frac{G(R_1, R_2)}{r^4}, \quad (29)$$

where $G(R_1, R_2)$ is defined in (29) and $G(R_1, R_2) = G(R_2, R_1) \geq 0$. $S_{A;B}$ is the mutual

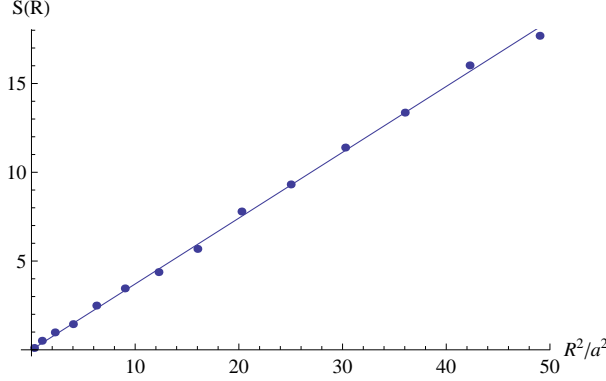


FIG. 1. The entanglement entropy $S(R)$ of one sphere whose radius is R as a function of R^2/a^2 . The line is the best linear fit.

information of A and B . From Fig.3 the approximate expression (29) is precise for relatively small r . (When $R_1 = R_2 \equiv R$, for $r \gtrsim 3R$ (29) is precise from Fig.3.) We can obtain $G(R_1, R_2)/a^4$ from slopes of graphs of $(S_A + S_B - S_{AB})^{-1/4}(r, R_1, R_2)$, and then we show the computed values of $G(R_1, R_2)/a^4$ as a function of R_2^2/a^2 for $R_1/a = 4, 4.5, \dots, 7$ in Fig.4. From Fig.4 we can see that $G(R_1, R_2)/a^4$ is proportional to R_2^2 . Because $G(R_1, R_2) = G(R_2, R_1)$, we obtain $G(R_1, R_2) = gR_1^2R_2^2$, where g is a dimensionless constant. We can obtain the values of gR_1^2 from slopes of graphs of $G(R_1, R_2)$ as a function of R_2^2 . To obtain the precise value of g , we show the computed values of gR_1^2/a^2 as a function of R_1^2/a^2 in Fig.5 and obtain $g = 0.26$ from the slope of the line which is the best linear fit in Fig.5.

Finally, when $r \gg R_1, R_2$, we obtain

$$-S_{A;B} = S_{AB}(r, R_1, R_2) - S_A(R_1) - S_B(R_2) \approx -\frac{0.26R_1^2R_2^2}{r^4}. \quad (30)$$

When $r \approx R_1, R_2$, from Fig.3, S_{AB} rapidly decreases when r decreases. (Note that we cannot determine the functional form of $G(R_1, R_2)$ only by the constraints from dimensional analysis, symmetry, and behavior in the limit $R_1 \rightarrow 0$. For example, $G(R_1, R_2) = R_1^3R_2 + R_1R_2^3$ is not prohibited by these constraints.)

For $d = 2$, we compute S_{AB} in the same way. We show only the computed values of $(S_A + S_B - S_{AB})^{-1/2}(r, R_1, R_2)$ as a function of r/a for $R_1/a = R_2/a = 15, 16$ in Fig.6. The straight lines in Fig.6 are fitted by the data between $r/a = R_1/a + R_2/a + 101$ and $r/a = R_1/a + R_2/a + 201$. In these regions the points are beautifully fitted by the straight lines. We cross-checked our numerical procedure with the data of related calculations in Figure 1 in [18]. (In the figure, the authors show the mutual information of two discs for

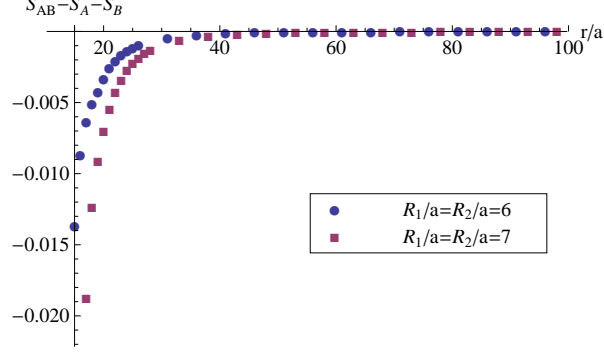


FIG. 2. $S_{AB} - S_A - S_B$ as a function of r/a for $R_1/a = R_2/a = 6, 7$, where S_{AB} is the entanglement entropy of two spheres A and B whose radii are R_1 and R_2 . The distance between the centers of the two spheres is r .

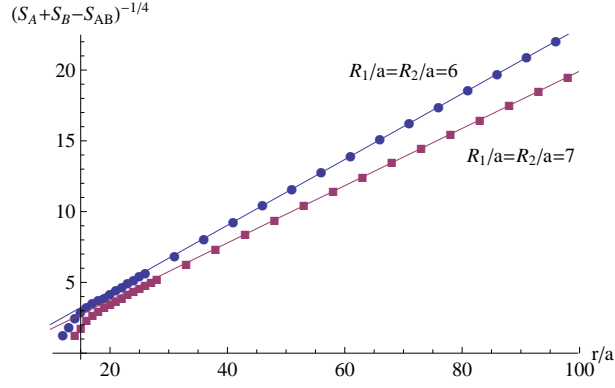


FIG. 3. $(S_A + S_B - S_{AB})^{-1/4}$ as a function of r/a for $R_1/a = R_2/a = 6, 7$, where S_{AB} is the entanglement entropy of two spheres A and B whose radii are R_1 and R_2 . The distance between the centers of the two spheres is r . The straight lines are fitted by the data between $r/a = R_1/a + R_2/a + 24$ and $r/a = R_1/a + R_2/a + 84$. For $r \gtrsim 3R (\equiv R_1 = R_2)$ the lines are beautifully fitted and the approximate expressions (29) and (30) are precise.

$R_1 = R_2 = R$ and $r = 3R$. Our results were very close to theirs.) Finally, when $r \gg R_1, R_2$, we obtain

$$-S_{A;B} = S_{AB}(r, R_1, R_2) - S_A(R_1) - S_B(R_2) \approx -\frac{0.37R_1R_2}{r^2}. \quad (31)$$

In order to examine whether only the degrees of freedom on the surface of the spheres contribute to the mutual information or not, we calculate the mutual information $S_{D;E}$ of two same spherical shells D and E for $d = 3$ and the mutual information $S_{H;I}$ of two same rings H and I for $d = 2$. The internal (external) radii of the spherical shell and the ring are L_1

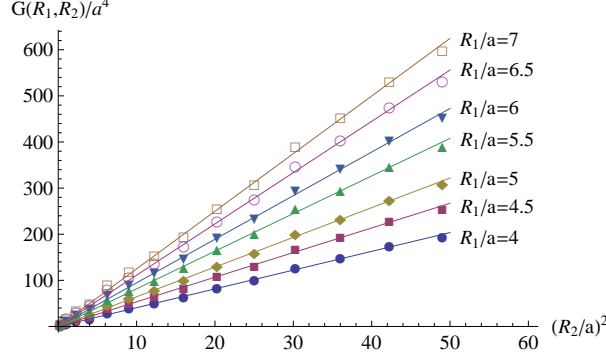


FIG. 4. $G(R_1, R_2)/a^4$ in (29) as a function of R_2^2/a^2 for $R_1/a = 4, 4.5, \dots, 7$. The lines are the best linear fit.

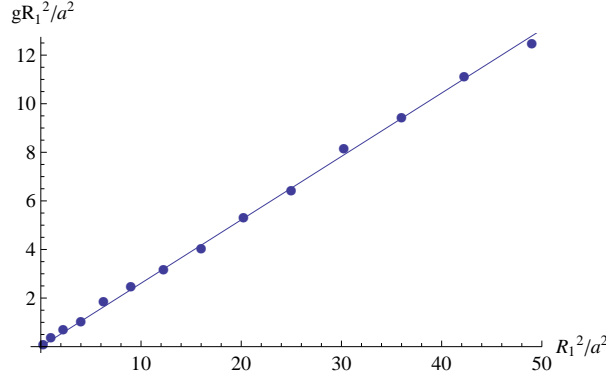


FIG. 5. gR_1^2/a^2 as a function of R_1^2/a^2 , where g is defined as $G(R_1, R_2) = gR_1^2R_2^2$. The line is the best linear fit.

(L_2). The distance between the centers of the two spherical shells and that between the two rings are r . When $r \gg L_2$, we obtain $S_{D;E} \approx G_{ss}(L_1, L_2)/r^4$ and $S_{H;I} \approx G_r(L_1, L_2)/r^2$. We show $(G_{ss}(L_1, L_2))^{1/2}/L_2^2$ for $L_2 = 10a$ as a function of L_1/L_2 in Fig.7 and $(G_r(L_1, L_2))^{1/2}/L_2$ for $L_2 = 22a$ as a function of L_1/L_2 in Fig.8. The curve in Fig.7 is $0.50(1 - (L_1/L_2)^3)^{2/3}$ and the curve in Fig.8 is $0.56(1 - (L_1/L_2)^2)^{1/2}$. We show these curves for comparison with the data. From Fig.7 and Fig.8, $(G_{ss}(L_1, L_2))^{1/2}/L_2^2$ and $(G_r(L_1, L_2))^{1/2}/L_2$ are monotone decreasing function of L_1/L_2 , and $(G_{ss}(L_1, L_2))^{1/2}$ is not proportional to the $2/3$ power of the volume of the spherical shell, and $(G_r(L_1, L_2))^{1/2}$ is not proportional to the $1/2$ power of the area of the ring. Then not only the degrees of freedom on the surface of the sphere but also those on the inside region contribute to the mutual information, and the degrees of freedom on the inside region does not contribute uniformly to the mutual information.

We roughly estimate the magnitude of the entropic force between two black holes by using

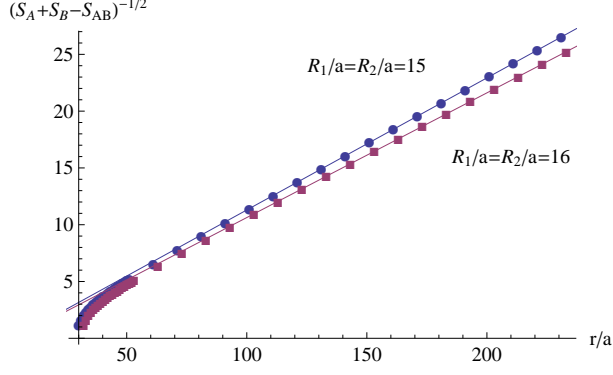


FIG. 6. $(S_A + S_B - S_{AB})^{-1/2}$ as a function of r/a for $R_1/a = R_2/a = 15, 16$, where S_{AB} is the entanglement entropy of two discs A and B whose radii are R_1 and R_2 . The distance between the centers of the two discs is r . The straight lines are fitted by the data between $r/a = R_1/a + R_2/a + 101$ and $r/a = R_1/a + R_2/a + 201$. For $r \gtrsim 4R (\equiv R_1 = R_2)$ the lines are beautifully fitted and the approximate expression (31) is precise.

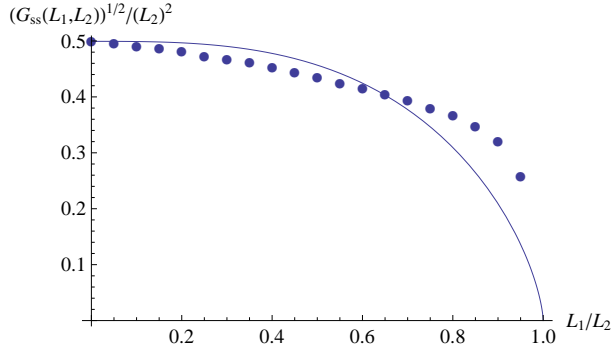


FIG. 7. $(G_{ss}(L_1, L_2))^{1/2}/L_2^2$ for $L_2 = 10a$ as a function of L_1/L_2 . $G_{ss}(L_1, L_2)$ is defined as $S_{D;E} \approx G_{ss}(L_1, L_2)/r^4$ when $r \gg L_1, L_2$. The curve is $0.50(1 - (L_1/L_2)^3)^{2/3}$. $(G_{ss}(L_1, L_2))^{1/2}/L_2^2$ is monotone decreasing function of L_1/L_2 and not proportional to $(1 - (L_1/L_2)^3)^{2/3}$.

S_{AB} in Minkowski spacetime. We consider two black holes (A and B) which have the same radius $R_1 = R_2 \equiv R$ and the distance between which is r . For simplicity, we consider the case that the state of the field on the whole space is a pure state. Generally, if a composite system XY is in a pure state, then $S_X = S_Y$ [13]. Then the entanglement entropy of the outside region of two black holes is equal to that of the inside regions of two black holes. We define the entropic force of the field on the outside region which acts on one black hole

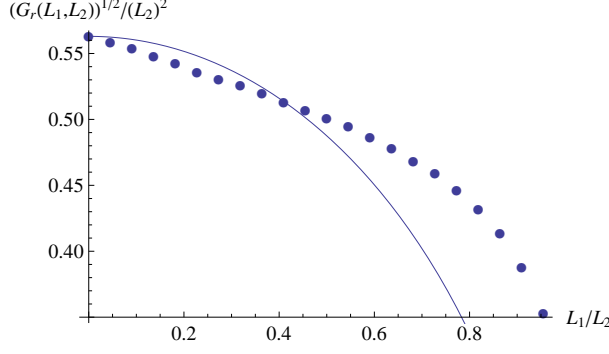


FIG. 8. $(G_r(L_1, L_2))^{1/2}/L_2^2$ for $L_2 = 22a$ as a function of L_1/L_2 . $G_r(L_1, L_2)$ is defined as $S_{H;I} \approx G_r(L_1, L_2)/r^2$ when $r \gg L_1, L_2$. The curve is $0.56(1 - (L_1/L_2)^2)^{1/2}$. $(G_r(L_1, L_2))^{1/2}/L_2^2$ is monotone decreasing function of L_1/L_2 and not proportional to $(1 - (L_1/L_2)^2)^{1/2}$.

in the direction of increasing r as F_{ef} . F_{ef} is given by

$$F_{ef} = T \frac{\partial S_{AB}}{\partial r}, \quad (32)$$

where T is the temperature of the field of the outside region. To estimate F_{ef} , we set S_{AB} to that in Minkowski spacetime and T to the Hawking temperature $T = (8\pi G_N M)^{-1} = (4\pi R)^{-1}$. In this approximation the entropic force is *repulsion force* because S_{AB} increases when r increases. $\partial S_{AB}/\partial r$ is independent of the ultraviolet cutoff, and then we obtain

$$F_{ef} = -\frac{T}{R} S'_{A;B}(r/R) = -\frac{1}{4\pi R^2} S'_{A;B}(r/R), \quad (33)$$

where $S_{A;B} = S_A(R) + S_B(R) - S_{AB}(r, R)$ and $S'_{A;B} \equiv \partial S_{A;B}/\partial(r/R)$. ($S_{A;B}$ is independent of the ultraviolet cutoff and a function of r/R .) Then the ratio of the entropic force to the force of gravity ($F_g = -\frac{G_N M^2}{r^2} = -\frac{R^2}{4G_N r^2}$) is

$$\left| \frac{F_{ef}}{F_g} \right| = \frac{1}{\pi} \left(\frac{l_P}{R} \right)^2 \left| \frac{S'_{A;B}(r/R)}{R^2/r^2} \right|, \quad (34)$$

where l_P is the Planck length $l_P = (G_N \hbar / c^3)^{1/2}$. When $r \gg R$, we substitute (30) into (34), and then we obtain

$$\left| \frac{F_{ef}}{F_g} \right| \approx 0.33 \left(\frac{l_P}{R} \right)^2 \frac{R^3}{r^3}. \quad (35)$$

When $r \approx R$, we show the computed values of $\left(\frac{R}{l_P} \right)^2 \left| \frac{F_{ef}}{F_g} \right|$ as a function of r/R for $R/a = 10$ in Fig.9. (Although from (34) $\left(\frac{R}{l_P} \right)^2 \left| \frac{F_{ef}}{F_g} \right|$ is a function of r/R and is independent of the choice of the value of R/a , the computed values of $\left(\frac{R}{l_P} \right)^2 \left| \frac{F_{ef}}{F_g} \right|$ slightly depend on the choice

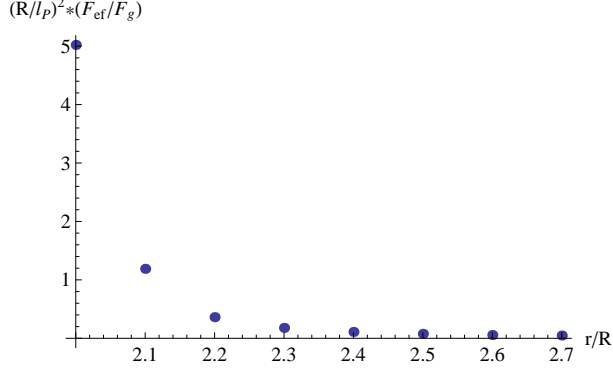


FIG. 9. The ratio of the entropic force to the force of gravity $\left(\frac{R}{l_P}\right)^2 \left|\frac{F_{ef}}{F_g}\right|$ as a function of r/R for $R/a = 10$.

of the value of R/a because the spheres on the lattice are distorted. When R/a is large, the spheres on the lattice are similar to the real spheres and this R/a dependence is small.) From (35) and Fig.9 the entropic force is much smaller than the force of gravity when $R \gg l_P$ and comparable to the force of gravity when $R \approx l_P$.

V. CONCLUSIONS AND DISCUSSION

We calculated numerically the entanglement entropy S_{AB} of two spheres and obtained the approximate expression (30). From Fig.3, (30) is precise for relatively small r . (When $R_1 = R_2 \equiv R$, for $r \gtrsim 3R$ (30) is precise from Fig.3.) We showed that the mutual information $S_{A;B}$ of A and B is independent of the ultraviolet cutoff for $d = 2, 3$ though S_A and S_B depends on the ultraviolet cutoff. The mutual information $S_{A;B}$ measures the entanglement between A and B and S_A measures the entanglement between A and A^c where A^c is the complementary of A . Then our results mean that the ultraviolet divergence of entanglement entropy in QFT is caused by the entanglement between points which are infinitely close to each other and the entanglement between regions which are finitely separate from each other is finite. And we showed that $S_{A;B}$ is the simple product of a function of R_1 and that of R_2 for $d = 2, 3$. These properties of $S_{A;B}$ for $d = 2, 3$ are most likely the same as those for $d \geq 4$. Then, from (1), for $d \geq 4$ when $r \gg R_1, R_2$ we assume

$$S_{A;B} \approx \frac{g_d R_1^{d-1} R_2^{d-1}}{r^{2d-2}}, \quad (36)$$

where $g_d \geq 0$ is a dimensionless constant.

In order to examine whether only the degrees of freedom on the surface of the spheres contribute to the mutual information or not, we calculate the mutual information $S_{D;E}$ of two same spherical shells D and E for $d = 3$ and the mutual information $S_{H;I}$ of two same rings H and I for $d = 2$. We obtained the result that not only the degrees of freedom on the surface of the sphere but also those on the inside region contribute to the mutual information, and the degrees of freedom on the inside region does not contribute uniformly to the mutual information. Because $S_{D;E}$ and $S_{H;I}$ measure the entanglement between regions which are finitely separate from each other, it is natural that the inside region contribute to the mutual information. The result that the inside region does not contribute uniformly to the mutual information means that the mutual information is not the product of the simple sum of the contribution from each volume elements. These results are different from that of the entanglement entropy to which the degrees of freedom on the surface of the boundary contribute mainly and uniformly. So the mutual information of two disconnected regions is not universally proportional to the product of the surface areas of the regions. Because a sphere has only one dimensionful parameter, the mutual information of two spheres is proportional to the product of the surface areas. For example, the mutual information of two rectangular solids is most likely not proportional to the product of the surface areas because a rectangular solid has three dimensionful parameters.

Our numerical method has three properties. First, we take the volume of the whole space to infinity, i.e. $N \rightarrow \infty$ in (17) and (18). Second, the computational complexity of our method depends only on the number of points on the regions of which we compute the entanglement entropy and does not depend on the distance between the separated regions. The computational complexity of conventional methods increases when the distance between the separated regions increases. This is because the numerical integrals of W_{mn} in (21) and W_{mn}^{-1} in (22) converge very slowly when $\|n - m\| \gg 1$. In order to reduce the computational complexity of W_{mn} and W_{mn}^{-1} , we use the approximate expressions (24) and (26) when $\|n - m\| > 10$. Third, we can compute the entanglement entropy of general shaped regions by our method because we do not use any symmetry of the regions of which we compute the entanglement entropy in our method. For example, we can compute the entanglement entropy of more than two separated regions. The first and the second properties enable us to obtain the r dependence of S_{AB} . And the third property enable us to compute S_{AB} for $R_1 \neq R_2$.

We estimated roughly the magnitude of the entropic force between two black holes. From (35) and Fig.9 the entropic force is comparable to the force of gravity when $R \approx l_P$. This rough estimate suggests that the entropic force is important for Planck scale black holes. (Of course, this result would be changed if the effect of quantum gravity would be taken into account when $R \approx l_P$.)

Next, we discuss the microscopic origin of the entropic force. As we see from (33) the entropic force is proportional to the r derivative of the mutual information $S_{A;B}$. So the origin of the entropic force is the entanglement between inside regions of two black holes. Due to the entanglement between inside regions of two black holes, the density matrix of the scalar field on the outside region changes when r changes. Then the force acts on black holes along the direction in which S_{AB} increases.

Finally we mention the validity of this estimate. When $r \gg R$, it is shown that $S_{A;B}$ in the black holes case can be expected to be similar to that in the Minkowski spacetime case except for the coefficient because almost all regions between two black holes is similar to Minkowski spacetime [12]. So, the rough estimate corresponds to the contribution to F_{ef} in (32) from $S_{A;B}$. However, in the black holes case S_A and S_B depend on r and contribute to F_{ef} . These contribution from S_A and S_B has been discussed in [12]. When $r \approx R$, $S_{A;B}$ in the black holes case is probably different from that in the Minkowski spacetime case because the region between two black holes is very different from Minkowski spacetime. However, even when $r \approx R$, $S_{A;B}$ is most likely independent of the ultraviolet cutoff as that in the Minkowski spacetime case.

ACKNOWLEDGMENTS

I am grateful to Takahiro Kubota and Satoshi Yamaguchi for a careful reading of this manuscript and useful comments and discussions. I also would like to thank Horacio Casini for informing me that I can cross-check my numerical procedure with the data of related calculations in [18]. This work was supported by a Grant-in-Aid from JSPS (No. 22-1930).

[1] L. Bombelli, R. K. Koul, J. Lee, and R. D. Sorkin, Phys. Rev. D34, 373 (1986)

[2] M. Srednicki, Phys. Rev. Lett. 71, 666 (1993), arXiv:hep-th/9303048

- [3] S. Hawking, J. M. Maldacena, and A. Strominger, JHEP 05, 001 (2001), arXiv:hep-th/0002145
- [4] D. N. Kabat, Nucl. Phys. B453, 281 (1995), arXiv:hep-th/9503016
- [5] L. Susskind and J. Uglum, Phys. Rev. D50, 2700 (1994), arXiv:hep-th/9401070
- [6] V. P. Frolov and I. Novikov, Phys. Rev. D48, 4545 (1993), arXiv:gr-qc/9309001
- [7] T. Jacobson, (1994), arXiv:gr-qc/9404039
- [8] G. 't Hooft, Nucl. Phys. B256, 727 (1985)
- [9] H. Casini and M. Huerta, JHEP 0903, 048 (2009), arXiv:0812.1773 [hep-th].
- [10] P. Calabrese, J. Cardy, and E. Tonni, J.Stat.Mech. 0911, P11001 (2009), arXiv:0905.2069 [hep-th].
- [11] P. Calabrese, J. Cardy, and E. Tonni, J.Stat.Mech. 1101, P01021 (2011), arXiv:1011.5482 [hep-th].
- [12] N. Shiba, Phys.Rev. D83, 065002 (2011), arXiv:1011.3760 [hep-th].
- [13] M. Nielsen and I. Chuang, *Quantum Computation and Quantum Information* (Cambridge University Press, Cambridge, England, 2000), p. 9.
- [14] P. Calabrese and J. L. Cardy, J. Stat. Mech. 0406, P002 (2004), arXiv:hep-th/0405152
- [15] C. Holzhey, F. Larsen, and F. Wilczek, Nucl. Phys. B424, 443 (1994), arXiv:hep-th/9403108
- [16] S. Ryu and T. Takayanagi, Phys. Rev. Lett. 96, 181602 (2006), arXiv:hep-th/0603001
- [17] S. Ryu and T. Takayanagi, JHEP 08, 045 (2006), arXiv:hep-th/0605073
- [18] H. Casini and M. Huerta, J. Phys. A42, 504007 (2009), arXiv:0905.2562 [hep-th]
- [19] S. N. Solodukhin, Living Rev.Rel. 14, 8 (2011), arXiv:1104.3712 [hep-th].
- [20] M. Creutz, *Quarks, gluons and lattices* (Cambridge Univ Pr, 1985).